Bulletin of Entomological Research (2016) **106**, 258–267
doi:10.1017/S0007485315001121

The life cycle of *Gregarina cuneata* in the midgut of *Tribolium castaneum* and the effects of parasitism on the development of insects

A.A.S. Gigliolli*, A.H.F. Julio and H. Conte

Departamento de Biotecnologia, Genética e Biologia Celular, Universidade Estadual de Maringá (UEM), Paraná, Brazil

Abstract

Tribolium castaneum Herbst 1797 (Coleoptera: Tenebrionidae), an important pest of stored grains and byproducts, is naturally infected by *Gregarina cuneata* Stein 1848 (Apicomplexa: Gregarinidae). Changes in the life cycle of insects caused by the parasite development in the midgut were studied. Trophozoites, gamonts (solitary and associated), and gametocysts were present in the midgut of the insects. In young trophozoites, the apical region differentiated into an epimerite that firmly attached the parasite to the host epithelial cells. With maturation, trophozoites developed in gamonts that were associated with the initiation of sexual reproduction in the cell cycle, culminating in the formation of the spherical gametocyst. Morpho-functional analyses indicated that gregarines absorb nutrients from infected cells and can occlude the midgut as they develop. Consequently, nutritional depletion may interfere with the host's physiology, causing decreased growth, delayed development, and high mortality rates of the parasitized insects. These results suggest *G. cuneata* could be an important biological agent for controlling *T. castaneum* in integrated pest management programs.

Keywords: *Tribolium castaneum*, Gregarines, morphology, developmental, mortality, control biological

(Accepted 21 December 2015; First published online 19 January 2016)

Introduction

Gregarines (Apicomplexa) are parasites of invertebrates, specifically annelids and arthropods. The life cycle includes oocyst ingestion, sporozoite release, trophozoite and gamont development, and gametocyst formation, which are released into the environment through feces (Clopton & Janovy, 1993).

These parasites can infect the fat body, Malpighian tubules, reproductive organs, hemolymph, and digestive system of various insect species (Schreurs & Janovy, 2008) and may cause adverse effects on the host's physiology, reproduction, longevity, and life cycle (Harry, 1970; Bouwma *et al*., 2005; Er & Gokce, 2005; Schreurs & Janovy, 2008; Lange & Lord, 2011; Lantova *et al*., 2011; Lord & Omoto, 2012).

Gregarina cuneata Stein 1848 (Eugregarinorida: Gregarinidae) naturally infects populations of *Tribolium castaneum* (Coleoptera: Tenebrionidae) as described by Ishii (1914), Hoshide (1979) and Gigliolli *et al*. (2015). This insect infests stored grains and by-products, causing quantitative and qualitative production losses (Smiderle, 2007).

The most common method used to control this insect is insecticide application; however, indiscriminate use has resulted in environmental bioaccumulation, development of insecticide-resistant insects, and toxic residue retention in stored grains and products. Given the economic impact of this insect in agriculture and commerce, the aim of this study was to analyze the morphofunctional features of *G. cuneata* development in the midgut of *T. castaneum* and its effect on the life cycle of parasitized insects, with the possibility of employing the parasite for the biological control of this pest,

*Author for correspondence
Phone: +55 44 30114466/ +55 44 99846378
E-mail: adrianasinopolis@hotmail.com

minimizing the impacts of chemical control agents on the environment and human health.

Material and methods

Insects

Adults of *T. castaneum* (60 female and 60 male >3 days old) naturally infected with *G. cuneata*, were obtained from breeding stocks of the Laboratory of Biological Control, Morphology and Cytogenetic of Insects at the Universidade Estadual de Maringa (23°25′30′′S and 51°56′20′′O), Parana, Brazil. The insects were kept at 30 ± 1°C, relative humidity of 70 ± 10%, 12 h photoperiod and fed on wheat flour.

Identification and characterization of gregarines in midgut

The insect hosts were cold anaesthetized, dissected in saline solution (0.1 M NaCl, 0.1 M Na_2HPO_4, and 0.1 M KH_2PO_4), and the alimentary canal was exposed. The organ was observed under a stereomicroscope (Zeiss) and the midgut was isolated and removed for anatomical characterization of gregarines located in this region.

For whole mount, the isolated midgut was stained using iodinated zinc chloride, then transferred to a glass slide and examined under a stereomicroscope (Zeiss) and light microscope (Olympus). Gregarines were photographed using a digital camera Sony Cyber Shot DSC 180.

Light microscopy

For histological characterization, the midguts of parasitized insects was fixed in aqueous Bouin's solution for 8 h. After dehydration in a series of increasing alcohol concentrations (70, 80, 90 and 100%), cleared in xylol, embedded in histological paraffin and cut into 6-µm-thick sections on Leica RM 2250 microtome. These sections were collected on glass slides, rehydrated, and stained with hematoxylin and eosin (H/E) and Periodic acid-Schiff (PAS) (Junqueira & Junqueira, 1983). Analyses were performed using a light microscope (Olympus), followed by photographic documentation.

Scanning electron microscopy (SEM)

For SEM, the midguts of insect parasitized were fixed in 2.5% glutaraldehyde in 0.1 M phosphate buffer (pH 7.3) for 48 h. They were then post-fixed in 1% osmium tetroxide in distilled water for 30 min and dehydrated in a series of increasing alcohol concentrations (Scudeler & Santos, 2013). The samples were critical-point dried (Leica CPD 030), coated with gold using a Shimadzu IC-50 coater, and observed using a Shimadzu SS-550 scanning electron microscope. The analyses of SEM were carried out in Microscopy Center of Complex Centers of Research Support (COMCAP) of the State University of Maringa, Parana, Brazil.

Transmission electron microscopy (TEM)

For TEM, portions of the midguts of parasitized insects were fixed in 2.5% glutaraldehyde and 4% paraformaldehyde in a 0.1 M phosphate buffer (pH 7.3) for 24 h. It was then post-fixed for 2 h without 1% osmium tetroxide in the same buffer, washed in distilled water and stained in 0.5% uranyl acetate for 2 h. Next, the sample was dehydrated in a series of increasing acetone concentrations and embedded in Araldite® resin. The ultrafine sections were stained in an alcoholic solution saturated with uranyl acetate and lead citrate (Scudeler & Santos, 2013) and observed under a JEOL JEM-1400 TEM. The analyses of TEM were carried out in Microscopy Center of Complex Centers of Research Support (COMCAP) of the State University of Maringa, Parana, Brazil.

Voucher specimens

Voucher specimens and the material analyzed were deposited at the Laboratory of Biological Control, Morphology and Cytogenetic of Insects at the Universidade Estadual de Maringa, Parana, Brazil.

Data analysis

The mortality and the size of the parasitized and unparasitized larvae were recorded at 8, 20, 31, 40, 48, and 59 days after hatching. χ^2 was used for independence ($\alpha = 0.05$), without Yates correction, and bilateral analysis was performed by analyzing differences in survival throughout the life cycle of *T. castaneum* individuals, for the control (unparasitized) and the parasitized groups. The normality of the lengths of the third-instar control and parasitized larvae were verified using the Shapiro–Wilk test ($\alpha = 0.05$). In the analysis of differences in length between third-instar control and parasitized larvae, the lengths were ranked for the Wilcoxon–Mann–Whitney test. All tests and graphics were generated using the software R version 3.0.2 with the stats package (R Core 144 Team, 2013).

Results

Morphology and development of G. cuneata *in the midgut of* T. castaneum

Trophozoites, gamonts (solitary and associated), and gametocysts were present in the midgut of the dissected insects (fig. 1).

In young trophozoites, the apical region was differentiated into an epimerite that firmly attached the parasite to the epithelial cells of the midgut during the extracellular development phase (fig. 2a, b).

The surface of the parasite's body was covered with straight or slightly undulated longitudinal pellicular folds known as epicytic folds (fig. 2a, b). These were formed by a trimembrane pellicle, which consists of the plasma membrane and the inner membrane complex formed by two adjacent cytomembranes (fig. 2c). There are electron-dense structures within apical parts of the epicytic folds called apical arcs and apical filaments (fig. 2c). Micropores are located between the epicytic folds and lead into invaginations of the plasma membrane inside the cytoplasm (fig. 2d, e). With development, there were changes in the density, size, and organization of the epicytic folds (figs 2a, b and 3a, b).

A septum divided the body into two segments: the protomerite and the deutomerite (fig. 2b). The protomerite, located above, remained in contact with the host's microvilli (fig. 3a). It varied from a cylindrical to an ovoidal shape and exhibited a slightly rounded anterior (fig. 3b–c). The anterior region presented a granular cytoplasm composed of amylopectin, a well-developed Golgi region, fibrils, and numerous electron-dense inclusions (fig. 3c–e). Maturing trophozoites and gamonts

https://doi.org/10.1017/S0007485315001121 Published online by Cambridge University Press

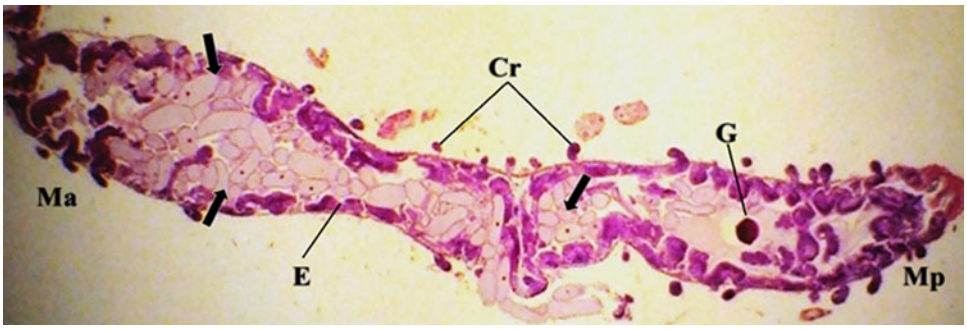

Fig. 1. Photomicrographs of *G. cuneata* in *T. castaneum* stained using H/E. Anterior region of the midgut (Ma); posterior region of the midgut (Mp); trophozoites and gamonts in the midgut (arrows); gametocyst in the posterior region of the midgut (G); regenerative crypts (Cr); epithelium (E). Scale bar = 20 µm.

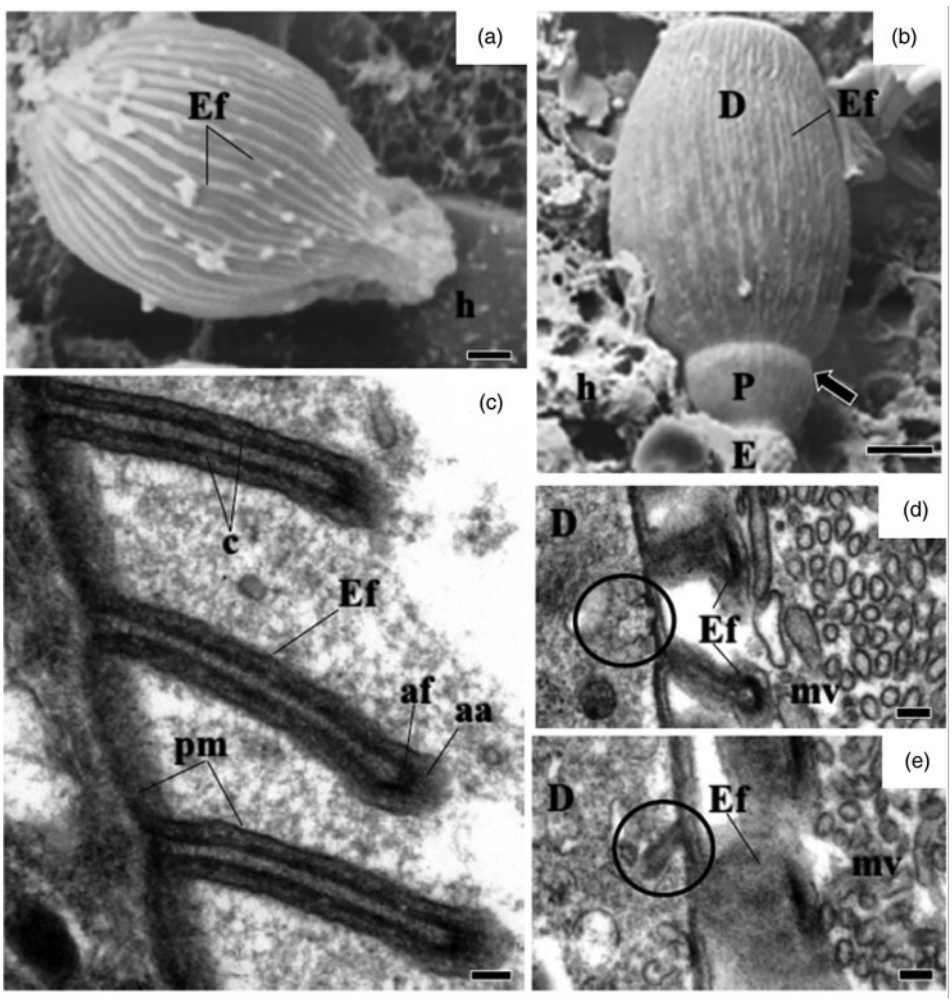

Fig. 2. Electron micrographs of development of *G. cuneata* in the midgut of adult *T. castaneum*. (a) SEM of non-segmented young trophozoite adhering to the epithelial cell (arrow). Host tissue (h); epicystic folds (Ef). Scale bar = 2 µm. (b) SEM of segmented young trophozoite. Epimerite (E); protomerite (P); deutomerite (D); epicystic folds (Ef); septum (arrow); host tissue (h). Scale bar = 5 µm. (c) TEM of epicystic folds (Ef). Plasma membrane (pm); cytomembranes (c); apical filaments (af); apical arcs (aa). Scale bar = 0.2 µm. (d) Micropore (circle); deutomerite (D); microvilli (mv); epicystic folds (Ef). Scale bar = 0.2 µm (e) Invaginations in internal lamina (circle); deutomerite (D); microvilli (mv); epicystic folds (Ef). Scale bar = 0.2 µm.

https://doi.org/10.1017/S0007485315001121 Published online by Cambridge University Press

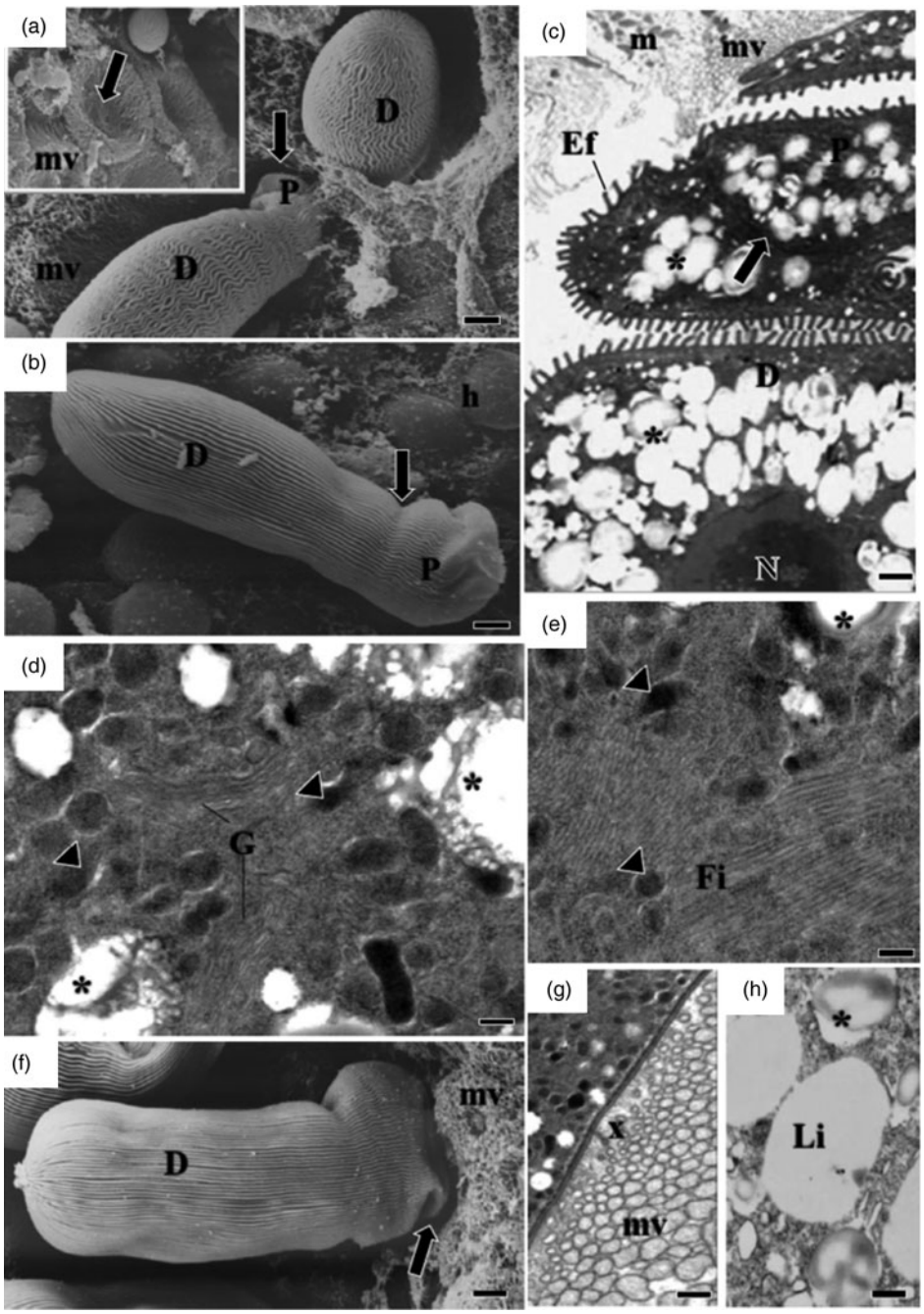

Fig. 3. Electron micrographs of mature trophozoites and gamonts of *G. cuneata*. (a) Trophozoites adhering to epithelial cells and detail of the invaginations formed in the microvilli after the release of trophozoites from the tissue (arrows). Microvilli (mv) deutomerite (D); protomerite (P). Scale bar = 2 µm. (b) SEM of trophozoites indicating protomerite (P) and deutomerite (D); septum (arrow); host cell (h). Scale bar = 2 µm. (c) Ultrastructure of maturing trophozoite. Septum (arrow); protomerite (P); deutomerite (D); microvilli (mv); epicytic folds (Ef); mitochondria (m); amylopectin granules (asterisk); nucleus (n). Scale bar = 5 µm. (d, e) Ultrastructure of the protomerite of maturing trophozoites. Electron-dense structure (arrowhead); Golgi region and vesicles (G); fibrils (Fi); amylopectin granules (asterisk). Scale bar = 0.2 µm. (f) SEM of the gamont. Deutomerite (D); projections in the protomerite (arrow); microvilli (mv). Scale bar = 2 µm. (h) TEM indicating deposition of amorphous material (x) between protomerite and microvilli (mv) of the host cell. Scale bar = 2 µm. (i) Lipid drops (L) and amylopectin granules (asterisk) in deutomerite. Scale bar = 0.2 µm.

developed projections similar to digitations in the protomerite (fig. 3f). It was noted the absence of epicytic folds and the presence of amorphous material of unknown origin in the contact zone between the host and the parasite (fig. 3g).

The elongated cylindrical deutomerite extended from the septum to the posterior region of the body; it increased in thickness and ended in a rounded extremity that abutted inside the midgut lumen (figs. 2a, b and 3a, b, f). A spherical

https://doi.org/10.1017/S0007485315001121 Published online by Cambridge University Press

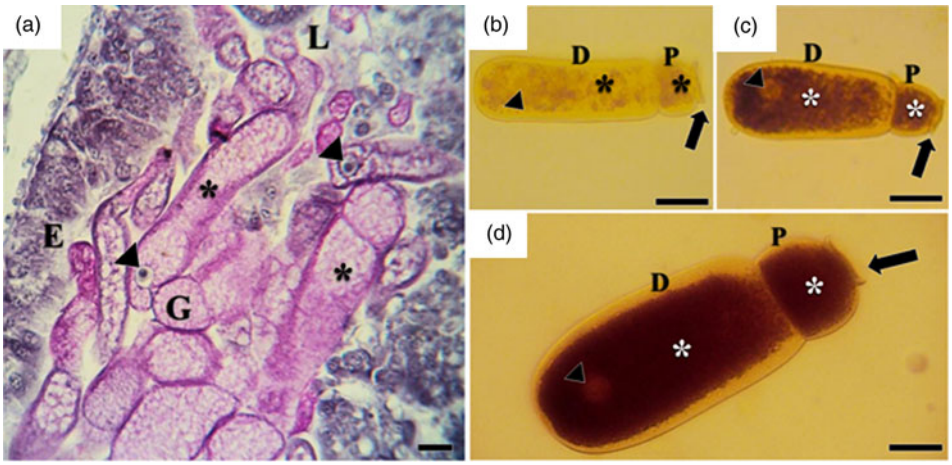

Fig. 4. Deposition of amylopectin granules during development of *G. cuneata*. (a) PAS positive gamonts (G) evident by the presence of amylopectin (asterisk); nucleus in the deutomerite (arrowhead); lumen (L); epithelium (E). Scale bar = 20 µm. (b–d) Total preparation of maturing trophozoites, stained with iodinated zinc chloride. Protomerite (P); deutomerite (D). Increased number of amylopectin granules deposited in the protomerite and deutomerite (asterisk); collar-like modified apical part of protomerite of the rather a detached satellite (arrows); nucleus (arrowhead); Scale bar = 20 µm.

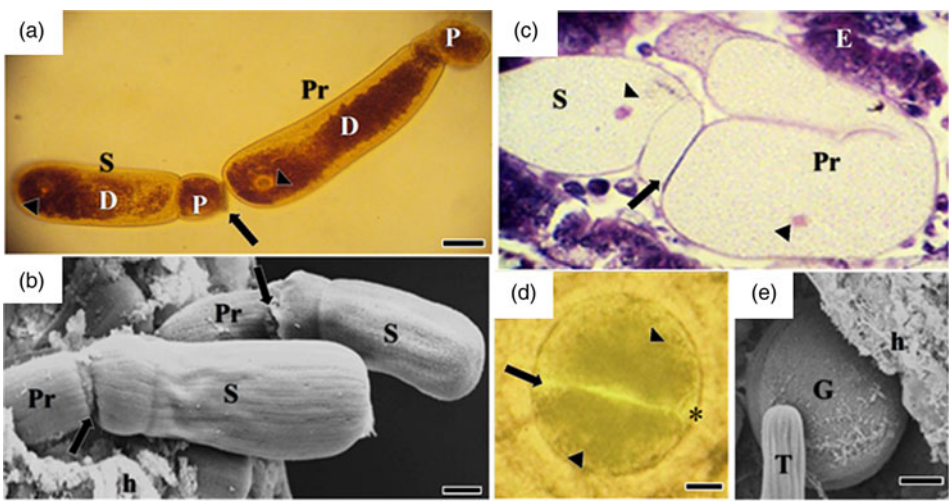

Fig. 5. Association of gamonts and gametocysts. (a) Recognition between sexual cells (arrow): primite (Pr) and satellite (S), stained with iodinated zinc chloride. Nucleus (arrowhead); protomerite (P); deutomerite (D). Scale bar = 20 µm. (b) SEM of associated primite (Pr) and satellite (S) gamonts adhering to the host tissue (h); Syzygy junction (arrow). primite (Pr); satellite (S); protomerite (P); deutomerite (D). Scale bar = 10 µm. (c) Satellite gamonts (S) and primite gamonts (Pr) initiating rotation movement, stained with H/E. Junctional complex (arrow); nucleus (arrowhead); epithelium (E). Scale bar = 20 µm. (d) Initial stage of gametocyst formation in which individual gamonts associate (arrow) to form a spherical structure, stained with iodinated zinc chloride. Nucleus (arrowhead), envelope and hyaline space (asterisk). (e) SEM of spherical gametocyst (G) located in the posterior region of the midgut (h). Trophozoite (T). Scale bar = 10 µm.

nucleus with a defined nucleolus, amylopectin granules (fig. 3c), and lipid droplets were located in this region (fig. 3h).

The amylopectin observed in both the protomerite and deutomerite were positively marked by PAS staining (fig. 4a). The number of granules deposited increased with maturation (fig. 4b, d).

Recognition between sexual cells initiated the reproduction phase (fig. 5a). In a biassociative and caudofrontal association, the anterior cell (primite) morphologically differed from the posterior cell (satellite). The primite exhibited a spatulate protomerite and an elongate cylindrical deutomerite; it became thicker furthest from the septum and had a rounded posterior extremity. The satellite had a hemispheric protomerite, and the deutomerite differed from the anterior cell only in length (fig. 5b, c).

Rotational movements and the morphological alterations observed in the associated gamonts (fig. 5c) resulted in the formation of spherical gametocysts (fig. 5d, e). These

https://doi.org/10.1017/S0007485315001121 Published online by Cambridge University Press

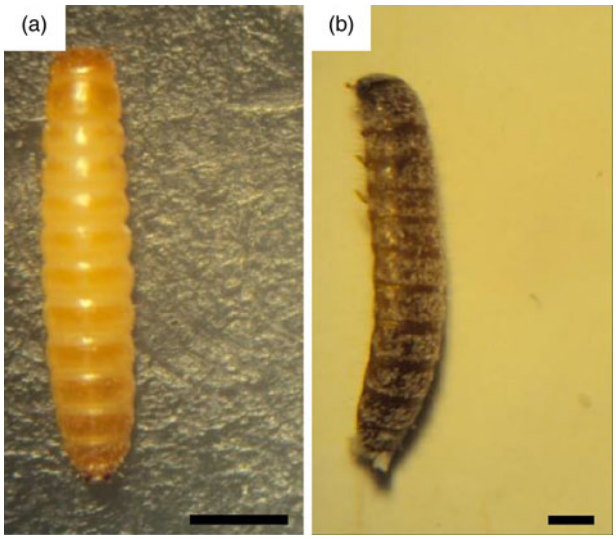

Fig. 6. Larvae of the *T. castaneum* with 31 days of the developmental. (a) Unparasitized, (b) parasitized. Scale bar = 1 mm.

structures were found in the posterior extremity of the midgut and in the proctodeum, from which they were released through the feces.

Development of T. castaneum *parasitized and unparasitized by* G. cuneata

We assessed the life cycle *T. castaneum*, parasitized and unparasitized (control) by *G. cuneata*. In both groups, the remaining eggs were incubated for 4 days; 42 parasitized and 40 unparasitized larvae hatched, and larval development was evaluated at 8, 20, 31, 40, 48, and 59 days after hatching.

The parasitized larvae showed blackened bodies and reduced size compared with unparasitized larvae (fig. 6).

This difference in length of parasitized ($W = 0.8496$, $P = 0.02814$) and unparasitized ($W = 0.6186$, $P = 9,513 \times 10^{-5}$) larvae at 31 days of development was initially assessed using the Shapiro–Wilk test (fig. 7). The results were not normally distributed and, thus, the non-parametric Wilcoxon–Mann–Whitney test was performed, showing a significant difference in the larval size in both groups ($W = 169$, $P = 9,825 \times 10^{-6}$, IC 95%: 1.999993–4.000041). The unparasitized larvae (5.2 mm average length) were larger than the parasitized larvae (3.7 mm average length) of the same age (fig. 8).

Using χ^2 independence, it was observed that the mortality of the parasitized larvae started after 8 days of development, and increased considerably at 20, 31, 40, 48, and 59 days, and it was significantly different to the unparasitized larvae (table 1, fig. 9a–f).

While 47.5% of the unparasitized larvae became pupae at 31 days, only one parasitized larvae reached this stage in the same period (fig. 9c). This was the only parasitized individual that reached the pupal stage in the whole period examined; however, it did not complete metamorphosis, dying 9 days after pupation (fig. 9d).

There was no insect emergence adult parasitized (fig. 9d–f). At 48 days of development, the mortality in this group reached 100% (fig. 9e). However, the unparasitized insects completed the cycle between 40 and 59 days after hatching,

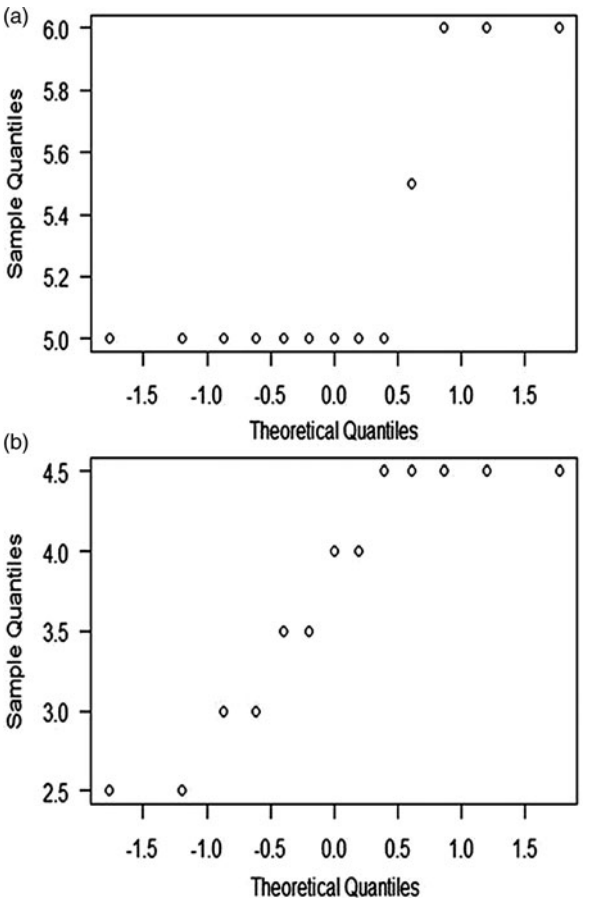

Fig. 7. Normal distribution of lengths *T. castaneum* larvae in third instar. (a) Unparasitized, (b) parasitized by *G. cuneata*.

and only 2.5% mortality was recorded in this period (table 1, fig. 9d–f).

Discussion

Tribolium castaneum is infected by *G. cuneata* after the ingestion of food containing oocysts and through cannibalism. Activation and excystation occur in the lumen of the midgut, in response to physiological stimuli such as the pH of intestinal contents, as observed in *Tenebrio molitor* infected by *G. cuneata* and *Gregarina polymorpha* (Clopton & Gold, 1995). The sporozoites, which were not assessed in this study, bind to midgut epithelial cells and develop into trophozoites.

At this stage, the parasites remained attached to the cells by an epimerite. In addition to attaching to the host, this structure is thought to be metabolically active and involved in gregarine feeding (Baudoin, 1969; Schrevel & Philippe, 1993; Valigurová *et al.*, 2009). The occurrence of endoplasmic reticulum and a large number of mitochondria in the apical region of infected cells suggests an interaction between the epimerite of *G. cuneata* and the epithelium of *T. castaneum*, as observed in *Didymorphyes gigantea* by Hildebrand (1976) and *Leidyana canadensis* by Lucarotti (2000).

When fixed to the host cell, the epimerite and protomerite cause deep invaginations in the plasma membrane of midgut

https://doi.org/10.1017/S0007485315001121 Published online by Cambridge University Press

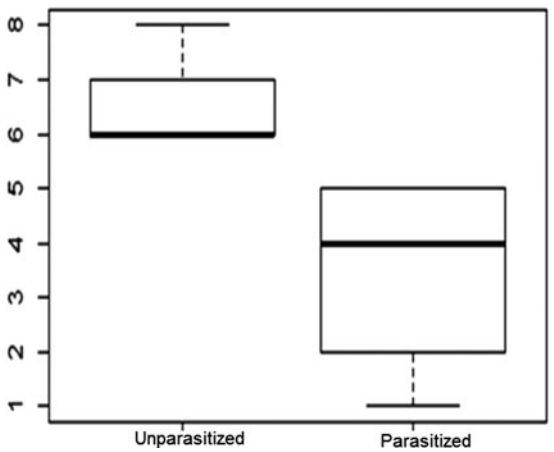

Fig. 8. Length of *T. castaneum* unparasitized and parasitized by *G. cuneata*. The *y*-axis is generated for ranking the Wilcoxon–Mann–Whitney test created with larval lengths, where 1 = 2.5, 2 = 3, 3 = 3.5, 4 = 4, 5 = 4.5, 6 = 5, 7 = 5.5, 8 = 6 cm.

epithelial cells in *T. castaneum* during larval development, similar to those observed in *Gregarina garnhami* infections of *Schistocerca gregaria* (Valigurová & Koudela, 2008) and *G. polymorpha* invasions of *T. molitor* larval intestines (Valigurová *et al.*, 2009).

According to Lucarotti (2000) and Valigurová *et al.* (2009), trophozoites can detach from senescent cells at any point and reattach to young cells, exhibiting better physiological conditions for the completion of their development. This is an active, self-regulated process involving gregarine motility (Walker *et al.*, 1979) and epimerite retraction, facilitated by contractile fibrils located in the epimerite itself and in the apical region of the protomerite (Lucarotti, 2000; Valigurová & Koudela, 2008; Valigurová *et al.*, 2009; Valigurová, 2012).

In the protomerite of *G. cuneata*, the presence of a fibril-rich region covered by an intact membrane, and the absence of epimerite remnants in the host tissue, may indicate the occurrence of the retraction mechanism observed previously in *G. cuneata* infections of *T. molitor* larvae by Valigurová (2012), in *G. garnhami* by Valigurová & Koudela (2008), in *G. polymorpha* by Valigurová *et al.* (2009), and in other parasitic species (Lucarotti, 2000; Heintzelman, 2004; Lange & Cigliano, 2004).

At the end of the growth period, the epimerite usually disappears and the gregarine cells acquire a dicystid-like morphology (protomerite and deutomerite). Projections similar to the digitations in the *G. cuneata* protomerite emerged and amorphous material accumulated at the interface between the parasitic anterior region and the microvilli of the host cell. The presence of a well-developed Golgi region and a large number of electron-dense vesicles in the protomerite must be related to the secretion of the amorphous, probably adhesive, substance (Valigurová *et al.*, 2007, 2008, 2009; Valigurová & Koudela, 2008; Valigurová, 2012).

Changes in the protomerite allowed mature trophozoites and gamonts to remain attached to the host where they possibly absorbed nutrients through a process based on membrane permeability (MacMillan, 1973; Valigurová & Koudela, 2008; Valigurová *et al.*, 2009; Valigurová, 2012).

The increasing deposition of amylopectin granules throughout *G. cuneata* development suggests an active metabolic interaction between the parasite and infected cells.

Table 1. Differences in survival *T. castaneum* parasitized and unparasitized by *G. cuneata* throughout its life cycle.

Developmental (days)	χ^2	df	*P*-value
8	7.2889	1	0.006938
20	17.484	1	2.897×10^{-5}
31	40.4938	1	1.972×10^{-10}
40	63.58	1	1.54×10^{-15}
48	70.7933	1	$<2.2 \times 10^{-16}$
59	70.7933	1	$<2.2 \times 10^{-16}$

Note: The results of 48 and 59 days are alike because no differences in mortality between unparasitized insects and parasitized insects, however, differences in the development stages were observed (see fig. 9e, f), df, degrees of freedom.

Gregarines must employ carbohydrates enzymatically degraded by the host to fuel energetically costly processes such as reproduction or motility (Schreurs & Janovy, 2008).

Gliding motility is driven by lateral undulations in the epicystic folds, through the action of either contractile proteins (Vivier, 1968; Valigurová *et al.*, 2013) or systems that antagonize fold filaments (Ruhl, 1976). Motility is alternatively achieved through the release of lubricating mucus (Schewiakoff, 1894; Valigurová *et al.*, 2013). In *G. cuneata*, micropore-like structures that interrupt the pellicle region may be involved in the secretion of mucus that facilitates motility (Schrevel, 1972; Talluri & Dallai, 1983).

In addition to their role in motility, fibrillar filaments in the apical extremity of the epicystic folds may be involved in morphological transformations that occur during gregarine development and culminate with the initiation of the sexual phase of the cycle (syzygy) and gametocyst formation (Toso & Omoto, 2007). These transformations are influenced by external factors such as temperature and humidity (Smith *et al.*, 2007), but mainly by the efficacy of the immune system (Thomas & Rudolf, 2010), diet, nutritional status (Rodriguez *et al.*, 2007; Schreurs & Janovy, 2008), and host physiology (Schawang & Janovy, 2001; Thomas & Rudolf, 2010).

Several studies have shown that physical and metabolic interactions established between parasites and their hosts are fundamental to the completion of their life cycle (Schawang & Janovy, 2001; Schreurs & Janovy, 2008). However, the pathogenicity of gregarines is still unknown and studies describing the effects of infection on reproduction, development, growth, longevity, and mortality of infected insects are limited (Harry, 1967; Dunkel & Boush, 1969; Schwalbe & Baker, 1976; Brooks & Jackson, 1990; Ball *et al.*, 1995; Johny *et al.*, 2000; Er & Gokce, 2005).

In the present study, parasitized larvae of *T. castaneum* decreased in size compared with unparasitized larvae of the same age, which may be indicate delayed growth. This impact may be associated with a reduction in food availability caused by occlusion of the midgut by the parasites during development, as seen in *Blattella germanica* (Lopes & Alves, 2005) and *Dermestes maculatus* (Lord & Omoto, 2012). Similarly, it may be associated with physical damage in the microvillis to the digestive cells which reduces absorption and excretion, causing host malnutrition as observed in *T. castaneum* adults parasitized by *G. cuneata* (Gigliolli *et al.*, 2015).

In addition to nutritional deficiencies, it is likely that other cell types as renegerative and endocrine cells are damaged, affecting hormone production and the regeneration of damaged tissue, as previously observed in *T. castaneum* parasitized by *G. cuneata* (Gigliolli *et al.*, 2015).

https://doi.org/10.1017/S0007485315001121 Published online by Cambridge University Press

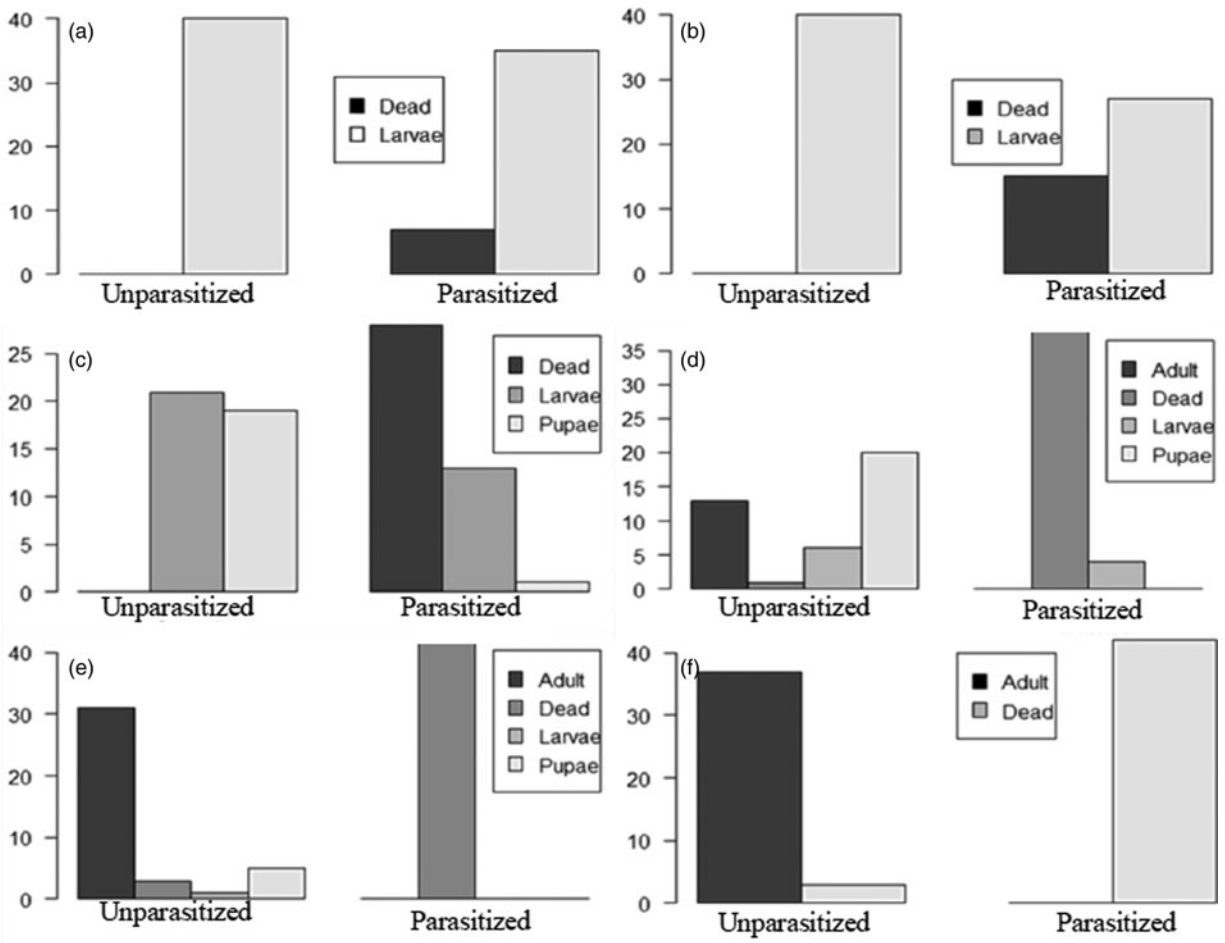

Fig. 9. Survival differences and delays in the development of *T. castaneum* unparasitized and parasitized by *G. cuneata* at different stages of development. (a) Insects with 8 days, (b) insects with 20 days, (c) insects with 31 days, (d) insects with 40 days, (e) insects with 48 days, and (f) insects 59 days of development.

These functional alterations in the midgut should be reflected in the insect physiology, interfering with metamorphosis or the ability of the larvae to molt, thereby hindering larval development and survival of the infected insects (Lucarotti, 2000; Valigurová & Koudela, 2005). As gregarine rapidly proliferate and frequently reinfect the same tissue, the insects lose their ability to repair damaged tissue and develop septicemia. This was observed in the high mortality rate of *B. germanica* parasitized by *Gregarina* sp. (Lopes & Alves, 2005).

Our results contradict those of Valigurová (2012) for studies on *T. molitor* parasitized by *G. cuneata*. While in *T. castaneum*, the infection resulted in morphological and physiological changes in the host (Gigliolli *et al.*, 2015), with negative impacts on their development and survival, in *T. molitor*, the same parasite might have favored the development, fitness, and survival of the parasitized insects (Valigurová, 2012).

Although *T. castaneum* and *T. molitor* are phylogenetically related species, and both can be infected by *G. cuneata*, the different pathogenic effects observed may be associated with the co-evolution of host and parasite. Although *T. castaneum* and *T. molitor* are phylogenetically related species, and both can be infected by *G. cuneata*, the different pathogenic effects observed may be associated with the co-evolution of host and parasite (Agnew *et al.*, 2000; Gourbal *et al.*, 2001; Lefèvre *et al.*, 2009).

In this evolutionary process, the parasite might have altered its morphophysiology and the host's (*T. molitor)* behavior to eliminate harmful relationships between members, thus encouraging the spread and survival of the parasite (Lefèvre *et al.*, 2009). The parasite may also have adapted to environmental conditions and other hosts physiochemical (*T. castaneum*), thereby establishing new evolutionary relationships.

For *G. cuneata* invasions, external environmental conditions, as well as morphological and physiological conditions of the host, can interfere with established relationships and have pathogenic effects on insects. This information allows us to evaluate new integrated pest management strategies and techniques that use natural enemies in storage units to reduce the proliferation of insects and, at the same time, resolve some of the environmental and health problems caused by conventional control methods.

Acknowledgments

We thank of the Centro de Microscopia Eletrônica (CME) at the Universidade Estadual Paulista (UNESP), Botucatu, SP

https://doi.org/10.1017/S0007485315001121 Published online by Cambridge University Press

and Centro de Microscopia (CMI) of Complexo de Centrais de Apoio à pesquisa (COMCAP) at the Universidade Estadual de Maringa (UEM), Maringa, PR in processing material used and assistance in handling the equipment. This work was supported by the Conselho Nacional de Desenvolvimento Científico e Tecnológico (CNPq).

References

Agnew, P., Koella, J.C. & Michelakis, Y. (2000) Host life history responses to parasitism. *Microbes and Infection* **2**, 891–896.

Ball, S.J., Cunningham, A.A., Clake, D. & Daszak, P. (1995) Septate gregarines associates with a disease of the hissing cockroach *Gromphadorhina portentosa*. *Journal of Invertebrate Pathology* **65**, 311–312.

Baudoin, J. (1969) On the ultrastructure of the anterior region of the gregarine *Ancyrophora puytoraci*. *Protistologica* **5**, 431–439.

Bouwma, A.J., Howard, K.J. & Jeanne, R.L. (2005) Parasitism in a social wasp: effect of gregarines on foraging behaviour, colony productivity, and adult mortality. *Behavioral Ecology Sociobiology* **59**, 222–233.

Brooks, W.M. & Jackson, J. (1990) Eugregarines: current status as pathogens, illustrated in corn rootworms. pp. 512–515 *in* Pinnock, D.E. (*Ed*.), *International Colloquium on Invertebrate Pathology and Microbial Control*. Adelaide, Australia.

Clopton, R.E. & Gold, R.E. (1995) Effects of pH on excystation in *G. cuneata* and *Gregarina polymorpha* (Eugregarinida: Gregarinidae). *Journal of Eukaryotic Microbiology* **42**, 540–544.

Clopton, R.E. & Janovy, J.J.R. (1993) Developmental niche structure in the gregarine assemblage parasitizing *Tenebrio molitor*. *Journal of Parasitology* **79**, 701–709.

Dunkel, F.V. & Boush, G.M. (1969) Effect of starvation on the black carpet beetle, *Attagenus megatoma*, infected with the eugregarine *Pyxinia frenzeli*. *Journal of Invertebrate Pathology* **14**, 49–52.

Er, M.K. & Gokce, A. (2005) Effect of *Diplocystis tipulae* sherlock (Eugregarinida: Apicomplexa), a coelomic gregarine pathogen of tipulids, on the larval size of *Tipula paludosa* meigen (Tipulidae: Diptera). *Journal of Invertebrate Pathology* **89**, 112–115.

Gigliolli, A.A.S., Lapenta, A.S., Ruvolo-Takasusuki, M.C.C., Abrahão, J. & Conte, H. (2015) Morpho-functional characterization and esterase patterns of the midgut of *T. castaneum* Herbst, 1797 (Coleoptera: Tenebrionidae) parasitized by *G. cuneata* (Apicomplexa: Eugregarinidae). *Micron* **76**, 68–78.

Gourbal, B.E.F., Righi, M., Petit, G. & Gabrion, C. (2001) Parasite-altered host behavior in the face of a predator: manipulation or not? *Parasitological Research* **87**, 186–192.

Harry, O.G. (1967) The effect of a eugregarine *Gregarina polymorpha* (Hammerschmidt) on the mealworm larva of *Tenebrio molitor* (L.). *Journal of Eukaryotic Microbiology* **14**, 539–547.

Harry, O.G. (1970) Gregarines: their effect on the growth of the desert locust (*Schistocerca gregaria*). *Nature* **225**, 964–966.

Heintzelman, M.B. (2004) Actin and myosin in *Gregarina polymorpha*. *Cell Motility and the Cytoskeleton* **58**, 83–95.

Hildebrand, H.F. (1976) Electron-microscopic investigation on evolution stages of trophozoite of *Didymophyes gigantea* (Sporozoa, Gregarinida). 1. Fine structure of protomerite and epimerite and relationship between host and parasite. *Parasitology Research* **49**, 193–215.

Hoshide, K. (1979) Notes on the gregarines in Japan 10. Three new and seventeen aldeady known species of gregarines from Japanese Tenebrionidae. *Bulletin of the Faculty of Education Yamaguchi University* **29**, 31–75.

Ishii, S. (1914) On four polycystid gregarines from the intestine of *Tribolium ferrugineum* F. *Annotationes Zoologicae Japonenses* **8**, 435–441.

Johny, S., Muralirangan, M.C. & Sanjayan, K.P. (2000) Parasitization portencial of two cephaline gregarines, *Leidyana Subramanii* Pushkala and Muralirangan and *Retractocephalus dhawanii* sp. N. on the Tobacco Grasshopper, *Atractomorpha crenulata* (FB.). *Journal of Orthoptera Research* **9**, 67–70.

Junqueira, L.C.U. & Junqueira, L.M.M.S. (*Eds*) (1983) *Técnicas básicas de citologia e histologia*, pp. 123. São Paulo, Livraria e Editora Santos.

Lange, C.E. & Cigliano, M.M. (2004) The life cycle of *Leidyana ampulla* sp. n. (Apicomplexa: Eugregarinorida: Leidyanidae) in the grasshopper *Ronderosia bergi* (Stal) (Orthoptera: Acrididae: Melanoplinae). *Acta Protozoologica* **43**, 81–87.

Lange, C. & Lord, J. (2011) Entomopathogenic protists. pp. 367–394 *in* Vega, F.E. & Kaya, H.K. (*Eds*) *Insect Pathology*. San Diego, Elsevier.

Lantova, L., Svobodova, M. & Volf, P. (2011) Effects of *Psychodiella sergenti* (Apicomplexa, Eugregarinorida) on its natural host *Phlebotomus sergenti* (Diptera, Psychodidae). *Journal of Medical Entomology* **48**, 985–990.

Lefèvre, T., Lebarbenchon, C., Gauthier-Clerc, M., Poulin, R. & Thomas, F. (2009) The ecological significance of manipulative parasites. *Trends in Ecological Evolution* **24**, 41–48.

Lopes, R.B. & Alves, S. (2005) Effect of *Gregarina* sp. parasitism on the susceptibility of *Blattella germanica* to some control agents. *Journal Invertebrate Pathology* **88**, 261–264.

Lord, J.C. & Omoto, C.K. (2012) Eugregarines reduce susceptibility of the hide beetle, *Dermestes maculatus*, to apicomplexan pathogens and retard larval development. *Journal of Invertebrate Pathology* **111**, 186–188.

Lucarotti, C.J. (2000) Cytology of *Leidyana canadensis* (Apicomplexa: Eugregarinida) in *Lambdina fiscellaria fiscellaria* larvae (Lepidoptera: Geometridae). *Journal of Invertebrate Pathology* **75**, 117–125.

MacMillan, W.G. (1973) Gregarine attachment organelles – structure and permeability of an interspecific cell junction. *Parasitology* **66**, 207–214.

R Core Team (2013). R: A language and environment for statistical computing. R Foundation for Statistical Computing, Vienna, Austria. Available online at http://www.R-project.org/

Rodriguez, Y., Omoto, C.K. & Gomulkiewicz, R. (2007) Individual and population effects of Eugregarine, *Gregarina niphandrodes* (Eugregarinida: Gregarinidae), on *Tenebrio molitor* (Coleoptera: Tenebrionidae). *Environmental Entomology* **36**, 689–693.

Ruhl, H. (1976) Contribution to the physiology of movement of gregarines: elements of movement, movement modes. *Zeitschrift für Parasitenkunde* **48**, 199–214.

Schawang, J.E. & Janovy, J.J.R. (2001) The response of *Gregarina niphandrodes* (Apicomplexa: Eugregarinida: Septatina) to host starvation in *Tenebrio molitor* (Coleoptera: Tenebrionidae) adults. *Journal of Parasitology* **87**, 600–605.

Schewiakoff, W. (1894) Uber die Ursache der fortschreitenden Bewegung der Gregarinen. *Zeitschrift für wissenschaftliche Zoologie* **58**, 340–354.

Schreurs, J. & Janovy, J.J.R. (2008). Gregarines on a diet: the effects of host Starvation on *Gregarina confusa* Janovy *et al*., 2007 (Apicomplexa: Eugregarinida) in *Tribolium destructor*

Uyttenboogaart, 1933 (Coleoptera: Tenebrionidae) Larvae. *Journal of Parasitology* **94**, 567–570.

Schrevel, J. (1972) Polysaccharides of cell-surface of gregarines (Protozoa Parasites). 1. Ultrastructure and cytochemistry. *Journal of Microscopy* **15**, 21–40.

Schrevel, J. & Philippe, M. (1993) The gregarines. pp. 133–245 *in* Kreier, J.P. (*Ed.*) *Parasitic Protozoa*. San Diego, Academic Press.

Schwalbe, C.P. & Baker, J.E. (1976) Nutrient reserves in starving black carpet beetle larvae infected with the eugregarine *Pyzinia frenzeli*. *Journal of Invertebrate Pathology* **28**, 11–15.

Scudeler, E.L. & Santos, D.C. (2013) Effects of neem oil (*Azadirachta indica* A. Juss) on midgut cells of predatory larvae *Ceraeochrysa claveri* (Navás, 1911) (Neuroptera: Chrysopidae). *Micron* **44**, 125–132.

Smiderle, O. (2007) Manejo integrado de pragas de grãos armazenados: identificação e controle. Artigo em Hypertexto. Available online at: http://www.infobibos.com/artigos/2007_2/pragasgraos/Index.htm (acesso em 06/03/2008).

Smith, A.J., Cook, T.J. & Lutterschmidt, W.I. (2007) Effects of temperature on the development of *Gregarina cubensis* (Apicomplexa: Eugregarinida) parasitizing *Blaberus discoidalis* (Blattaria: Blaberidae). *Journal of Parasitology* **93**, 583–588.

Talluri, M.V. & Dallai, R. (1983) Freeze-fracture study of the gregarine trophozoite: II. Evidence of ''rosette'' organization on cytomembranes in relation with micropore structure. *Bollettino di Zoologia* **50**, 247–256.

Thomas, A.M. & Rudolf, V.H.W. (2010) Challenges of metamorphosis in invertebrate hosts: maintaining parasite resistance across life-history stages. *Ecological Entomology* **35**, 200–205.

Toso, M.A. & Omoto, C.K. (2007) Ultrastructure of the *Gregarina niphandrodes* nucleus through stages from unassociated trophozoites to gamonts in syzygy and the syzygy junction. *Journal of Parasitology* **93**, 479–484.

Valigurová, A. (2012) Sophisticated adaptations of *G. cuneata* (Apicomplexa) feeding stages for Epicellular parasitism. *PLoS ONE* **7**, 1–11.

Valigurová, A. & Koudela, B. (2005) Fine structure of trophozoites of the gregarine *Leidyana ephestiae* (Apicomplexa: Eugregarinida) parasitic in *Ephestia kuehniella* larvae (Lepidoptera). *European Journal of Protistology* **41**, 209–218.

Valigurová, A. & Koudela, B. (2008) Morphological analysis of the cellular interactions between the eugregarine *Gregarina garnhami* (Apicomplexa) and the epithelium of its host, the desert locust *Schistocerca gregaria*. *European Journal of Protistology* **44**, 197–207.

Valigurová, A., Hofmannova, L., Koudela, B. & Vavra, J. (2007) An ultrastructural comparison of the attachment sites between *Gregarina steini* and *Cryptosporidium muris*. *Journal of Eukaryotic Microbiology* **54**, 495–510.

Valigurová, A., Jirku, M., Koudela, B., Gelnar, M., Modry, D. & Slapeta, J. (2008) Cryptosporidia: epicellular parasites embraced by the host cell membrane. *International Journal for Parasitology* **38**, 913–922.

Valigurová, A., Michalkova, V. & Koudela, B. (2009) Eugregarine trophozoite detachment from the host epithelium via epimerite retraction: fiction or fact? *International Journal for Parasitology* **39**, 1235–1242.

Valigurová, A., Vaškovicová, N., Musilová, N. & Schrével, J. (2013) The enigma of eugregarine epicytic folds: where gliding motility originates? *Frontiers in Zoology* **10**, 2–27.

Vivier, E. (1968) L'organisation ultrastructurale corticale de la Gregarine *Lecudina pellucida*; ses rapports avec l'alimentation et la locomotion. *Journal of Protozoology* **15**, 230–246.

Walker, M.H., Mackenzie, C., Bainbridge, S.P. & Orme, C. (1979) A study of the structure and gliding movement of *Gregarina garnhami*. *Journal of Protozoology* **26**, 566–574.

https://doi.org/10.1017/S0007485315001121 Published online by Cambridge University Press